# Electronic Supplementary Information

for

## Is histidine dissociation a critical component of the NO/H-NOX signaling mechanism? Insights from X-ray absorption spectroscopy

Zhou Dai,[a,c] Erik R. Farquhar,[b] Dhruv P. Arora,[a] and Elizabeth M. Boon*[a]

**Contents:**

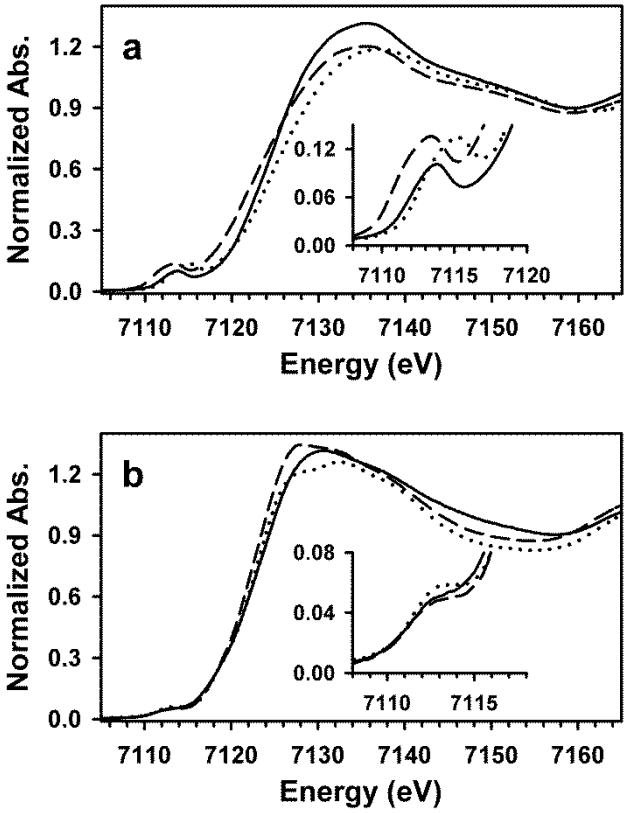


**Figure S1.** XANES spectra of the NO-bound (a, top panel) and Fe(II)-unligated (b, bottom panel) states of H-NOX from *Tt* (solid lines), *Sw* (dashed lines), and *Pa* (dotted lines). The insets depict an expansion of the pre-edge transition for each sample.

**Table S1.** Selected EXAFS fits to the NO-bound state of *Sw* H-NOX.[a]

| ***S.w.* H-NOX Fe(II)-NO** | | | | | | | | | | | | |
|---|---|---|---|---|---|---|---|---|---|---|---|---|
| **fit 1** | | | **fit 2** | | | **fit 3** | | | **fit 4** | | | |
| shell | r | $\sigma^2$ | shell | r | $\sigma^2$ | shell | r | $\sigma^2$ | shell | r | $\sigma^2$ |
| | | | 1 Fe-NO | 1.75 | 1.8 | 1 Fe-NO | 1.75 | 0.4 | 1 Fe-NO | 1.75 | 2.1 |
| 4 Fe-$N_p$ | 2.00 | 1.9 | 4 Fe-$N_p$ | 1.99 | 2.0 | 4 Fe-$N_p$ + 1 Fe-$N_{His}$ | 1.99 | 3.8 | 4 Fe-$N_p$ | 1.99 | 2.1 |
| | | | | | | | | | 1 Fe-$N_{His}$ | 2.32 | 8.4 |
| 8 Fe••Cα | 3.02 | 3.0 | 8 Fe••Cα | 3.02 | 3.0 | 8 Fe••Cα | 3.02 | 3.0 | 8 Fe••Cα | 3.02 | 3.0 |
| 16 Fe••Cα/$N_p$ | 3.20 | 6.1 | 16 Fe••Cα/$N_p$ | 3.19 | 6.1 | 16 Fe••Cα/$N_p$ | 3.19 | 6.1 | 16 Fe••Cα/$N_p$ | 3.19 | 6.1 |
| 4 Fe••$C_h$ | 3.39 | 2.4 | 4 Fe••$C_h$ | 3.38 | 3.5 | 4 Fe••$C_h$ | 3.38 | 3.5 | 4 Fe••$C_h$ | 3.38 | 3.2 |
| 8 Fe••Cβ | 4.38 | 5.0 | 8 Fe••Cβ | 4.36 | 4.8 | 8 Fe••Cβ | 4.36 | 5.1 | 8 Fe••Cβ | 4.36 | 4.7 |
| 16 Fe••Cβ/$N_p$ | 4.41 | 10.1 | 16 Fe••Cβ/$N_p$ | 4.39 | 9.6 | 16 Fe••Cβ/$N_p$ | 4.39 | 10.2 | 16 Fe••Cβ/$N_p$ | 4.39 | 9.4 |
| F | | 0.468 | F | | 0.342 | F | | 0.389 | F | | 0.321 |
| $\Delta E_0$ | | 9.20 | $\Delta E_0$ | | 7.65 | $\Delta E_0$ | | 7.62 | $\Delta E_0$ | | 7.70 |

[a] *r* is in units of Å; $\sigma^2$ is in units of $10^{-3}$ Å$^2$; $\Delta E_0$ is in units of eV. All fits are to unfiltered data. F represents a goodness-of-fit parameter. Fourier transform range of $k$ = 2.0 – 13.85 Å$^{-1}$ (resolution = 0.134 Å). Values of r for the Fe••Cα single scattering and Fe••Cα/$N_p$ multiple scattering paths were constrained to a constant difference from one another, while $\sigma^2$ for the multiple scattering path was constrained to be twice that of the single scattering path. A similar constraint was placed on the Cβ and Cβ/$N_p$ combination.

**Table S2.** Selected EXAFS fits to the NO-bound state of *Pa* H-NOX.[a]

| ***P.a.* H-NOX Fe(II)-NO** | | | | | | | | | | | | |
|---|---|---|---|---|---|---|---|---|---|---|---|---|
| **fit 1** | | | **fit 2** | | | **fit 3** | | | **fit 4** | | | |
| shell | r | $\sigma^2$ | shell | r | $\sigma^2$ | shell | r | $\sigma^2$ | shell | r | $\sigma^2$ | |
| | | | 1 Fe-NO | 1.72 | 5.3 | 1 Fe-NO | 1.71 | 2.9 | 1 Fe-NO | 1.72 | 5.4 | |
| 4 Fe-$N_p$ | 1.99 | 4.4 | 4 Fe-$N_p$ | 1.98 | 4.0 | 4 Fe-$N_p$ + 1 Fe-$N_{His}$ | 1.97 | 6.1 | 4 Fe-$N_p$ | 1.98 | 4.0 | |
| | | | | | | | | | 1 Fe-$N_{His}$ | 2.35 | 10.5 | |
| 8 Fe••Cα | 3.04 | 2.6 | 8 Fe••Cα | 3.03 | 2.8 | 8 Fe••Cα | 3.03 | 2.8 | 8 Fe••Cα | 3.03 | 2.7 | |
| 16 Fe••Cα/$N_p$ | 3.21 | 5.1 | 16 Fe••Cα/$N_p$ | 3.20 | 5.6 | 16 Fe••Cα/$N_p$ | 3.20 | 5.7 | 16 Fe••Cα/$N_p$ | 3.20 | 5.5 | |
| 8 Fe••Cβ | 4.41 | 8.8 | 8 Fe••Cβ | 4.37 | 7.1 | 8 Fe••Cβ | 4.36 | 6.8 | 8 Fe••Cβ | 4.36 | 6.7 | |
| 16 Fe••Cβ/$N_p$ | 4.44 | 17.7 | 16 Fe••Cβ/$N_p$ | 4.39 | 14.2 | 16 Fe••Cβ/$N_p$ | 4.39 | 13.7 | 16 Fe••Cβ/$N_p$ | 4.39 | 13.4 | |
| F | | 0.492 | F | | 0.406 | F | | 0.442 | F | | 0.393 | |
| $\Delta E_0$ | | 8.54 | $\Delta E_0$ | | 6.21 | $\Delta E_0$ | | 5.84 | $\Delta E_0$ | | 5.82 | |

[a] *r* is in units of Å; $\sigma^2$ is in units of $10^{-3}$ Å$^2$; $\Delta E_0$ is in units of eV. All fits are to unfiltered data. F represents a goodness-of-fit parameter. Fourier transform range of $k$ = 2.0 – 12.5 Å$^{-1}$ (resolution = 0.150 Å). Values of r for the Fe••Cα single scattering and Fe••Cα/$N_p$ multiple scattering paths were constrained to a constant difference from one another, while $\sigma^2$ for the multiple scattering path was constrained to be twice that of the single scattering path. A similar constraint was placed on the Cβ and Cβ/$N_p$ combination. Inclusion of the Fe••$C_h$ single scattering paths for the heme meso carbons was not required.

**Table S3.** Selected EXAFS fits to the Fe(II)–unligated state of *Sw* H-NOX.[a]

| ***S.w.* H-NOX Fe(II)-unligated** | | | | | | | | | | | | |
|---|---|---|---|---|---|---|---|---|---|---|---|---|
| **fit 1** | | | **fit 2** | | | **fit 3** | | | **fit 4** | | | |
| shell | r | $\sigma^2$ | shell | r | $\sigma^2$ | shell | r | $\sigma^2$ | shell | r | $\sigma^2$ |
| 4 Fe-$N_p$ | 2.07 | 4.0 | 4 Fe-$N_p$ + 1 Fe-$N_{His}$ | 2.06 | 5.7 | 4 Fe-$N_p$ | 2.07 | 4.0 | 4 Fe-$N_p$ + 1 Fe-$N_{His}$ | 2.07 | 5.8 |
| | | | | | | 1 Fe-$N_{His}$/O | 2.67 | 14.3 | 1 Fe-O | 2.61 | 17.6 |
| 8 Fe••Cα | 3.11 | 6.1 | 8 Fe••Cα | 3.11 | 6.6 | 8 Fe••Cα | 3.10 | 6.3 | 8 Fe••Cα | 3.10 | 6.9 |
| 4 Fe••$C_h$ | 3.41 | 1.0 | 4 Fe••$C_h$ | 3.41 | 0.55 | 4 Fe••$C_h$ | 3.42 | 0.9 | 4 Fe••$C_h$ | 3.41 | 0.5 |
| 8 Fe••Cβ | 4.43 | 4.0 | 8 Fe••Cβ | 4.42 | 3.8 | 8 Fe••Cβ | 4.43 | 4.0 | 8 Fe••Cβ | 4.42 | 3.8 |
| 16 Fe••Cβ/$N_p$ | 4.46 | 7.9 | 16 Fe••Cβ/$N_p$ | 4.45 | 7.6 | 16 Fe••Cβ/$N_p$ | 4.46 | 8.0 | 16 Fe••Cβ/$N_p$ | 4.45 | 7.65 |
| F | | 0.276 | F | | 0.301 | F | | 0.261 | F | | 0.287 |
| $\Delta E_0$ | | 4.40 | $\Delta E_0$ | | 3.88 | $\Delta E_0$ | | 4.62 | $\Delta E_0$ | | 4.12 |

[a] *r* is in units of Å; $\sigma^2$ is in units of $10^{-3}$ $Å^2$; $\Delta E_0$ is in units of eV. All fits are to unfiltered data. F represents a goodness-of-fit parameter. Fourier transform range of $k$ = 2.0 – 12.0 $Å^{-1}$ (resolution = 0.157 Å). Values of r for the Fe••Cβ single scattering and Fe••Cβ/$N_p$ multiple scattering paths were constrained to a constant difference from one another, while $\sigma^2$ for the multiple scattering path was constrained to be twice that of the single scattering path. Inclusion of the Fe••Cα/$N_p$ multiple scattering paths was not required.

**Table S4.** Selected EXAFS fits to the Fe(II)–unligated state of *Pa* H-NOX.[a]

| ***P.a.* H-NOX Fe(II)-unligated** | | | | | | | | | | | | |
|---|---|---|---|---|---|---|---|---|---|---|---|---|
| **fit 1** | | | **fit 2** | | | **fit 3** | | | **fit 4** | | | |
| shell | r | $\sigma^2$ | shell | r | $\sigma^2$ | shell | r | $\sigma^2$ | shell | r | $\sigma^2$ |
| 4 Fe-$N_p$ | 2.06 | 3.6 | 4 Fe-$N_p$ + 1 Fe-$N_{His}$ | 2.06 | 5.2 | 4 Fe-$N_p$ | 2.06 | 3.7 | 4 Fe-$N_p$ + 1 Fe-$N_{His}$ | 2.06 | 5.2 |
| | | | | | | 1 Fe-$N_{His}$/O | 2.67 | 20.4 | 1 Fe-O | 2.57 | 25.5 |
| 8 Fe••Cα | 3.10 | 3.2 | 8 Fe••Cα | 3.10 | 3.1 | 8 Fe••Cα | 3.10 | 3.1 | 8 Fe••Cα | 3.10 | 3.1 |
| 4 Fe••$C_h$ | 3.41 | 2.1 | 4 Fe••$C_h$ | 3.40 | 2.37 | 4 Fe••$C_h$ | 3.41 | 2.2 | 4 Fe••$C_h$ | 3.41 | 2.3 |
| 8 Fe••Cβ | 4.43 | 3.7 | 8 Fe••Cβ | 4.42 | 3.9 | 8 Fe••Cβ | 4.43 | 3.7 | 8 Fe••Cβ | 4.43 | 3.8 |
| 16 Fe••Cβ/$N_p$ | 4.45 | 7.4 | 16 Fe••Cβ/$N_p$ | 4.45 | 7.7 | 16 Fe••Cβ/$N_p$ | 4.46 | 7.5 | 16 Fe••Cβ/$N_p$ | 4.45 | 7.65 |
| F | | 0.283 | F | | 0.306 | F | | 0.272 | F | | 0.295 |
| $\Delta E_0$ | | 3.63 | $\Delta E_0$ | | 3.31 | $\Delta E_0$ | | 3.86 | $\Delta E_0$ | | 3.66 |

[a] *r* is in units of Å; $\sigma^2$ is in units of $10^{-3}$ Å$^2$; $\Delta E_0$ is in units of eV. All fits are to unfiltered data. F represents a goodness-of-fit parameter. Fourier transform range of $k$ = 2.0 – 13.0 Å$^{-1}$ (resolution = 0.142 Å). Values of r for the Fe••Cβ single scattering and Fe••Cβ/$N_p$ multiple scattering paths were constrained to a constant difference from one another, while $\sigma^2$ for the multiple scattering path was constrained to be twice that of the single scattering path. Inclusion of the Fe••Cα/$N_p$ multiple scattering paths was not required.